SUPPLEMENTARY DATA

RGG-box in hnRNPA1 specifically recognizes the telomere G-quadruplex DNA and enhances the G-quadruplex unfolding ability of UP1 domain

Meenakshi Ghosh[1] and Mahavir Singh[1,2,*]

[1]Molecular Biophysics Unit, Indian Institute of Science, Bengaluru, 560012

[2]NMR Research Centre, Indian Institute of Science, Bengaluru, 560012

* To whom correspondence should be addressed

Tel: +91 80 2293 2839; Fax: +91 80 2293 2839; Email: singh@iisc.ac.in

Overview:

Figure S1

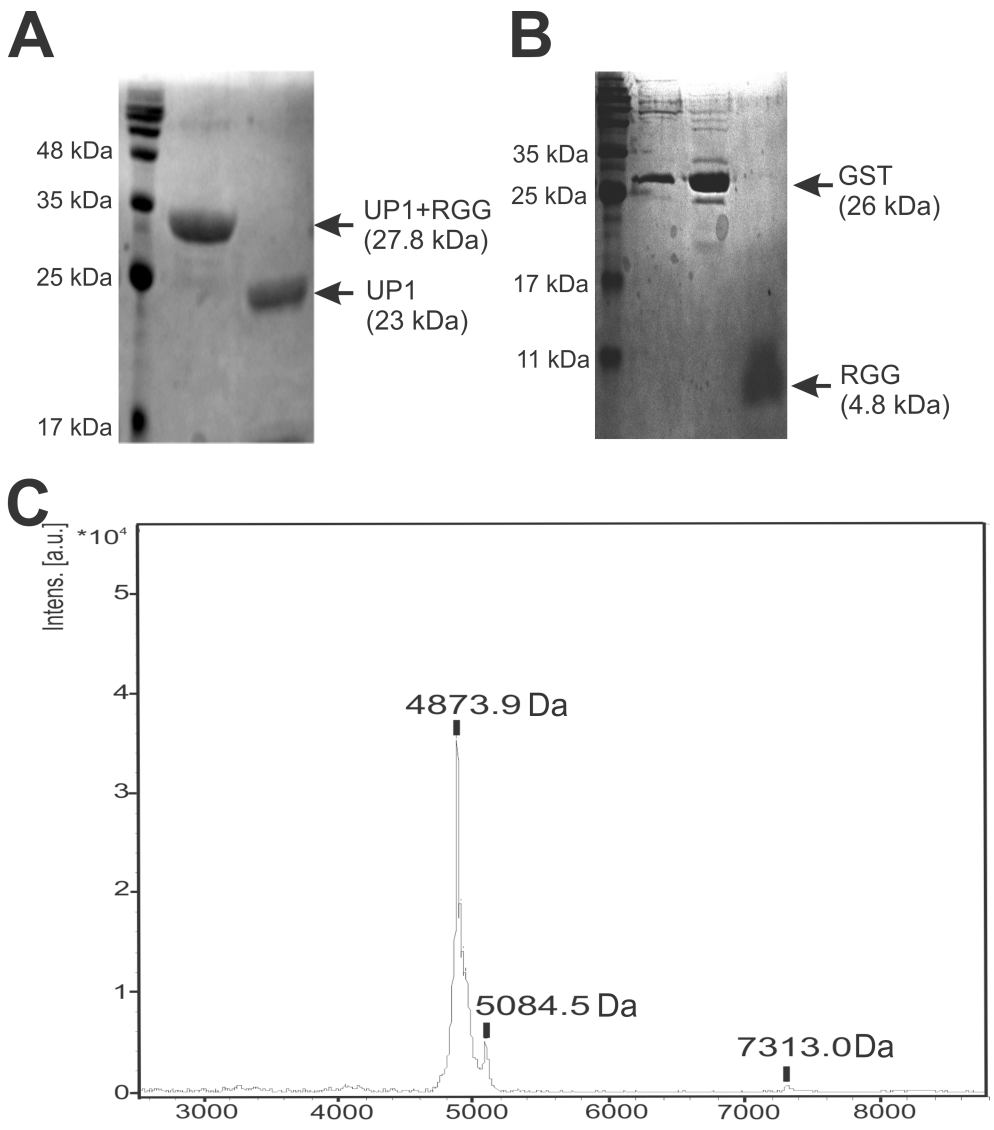

SI Figure 1. Purification of the proteins used in this study. **(A)** SDS PAGE showing purified UP1 and UP1+RGG proteins. **(B)** SDS PAGE of purified RGG-box after removal of GST-tag and size exclusion chromatography. **(C)** The mass of the RGG-box was further confirmed by MALDI –TOF MS analysis.

Figure S2

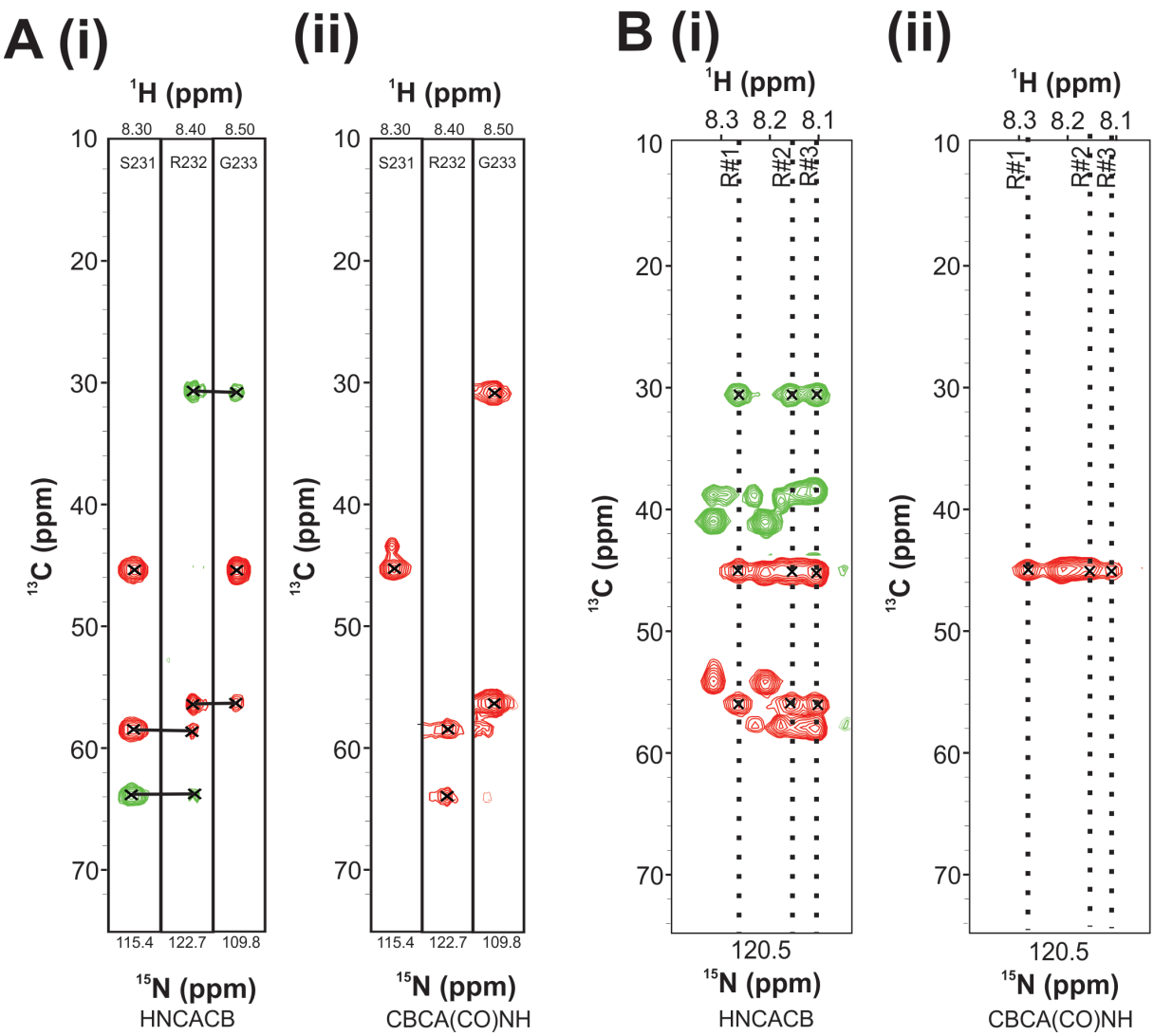

SI Figure 2. Strip plots showing NMR resonance assignment of the residues present in the RGG-box. **(A) (i)** HNCACB and **(ii)** CBCA(CO)NH strip plots showing sequential assignment of S231, R232, and G233 residues of the RGG-box. **(B i, ii)** The peaks pertaining to the arginine residues could be identified based on the chemical shift values for the residues and by the presence of the preceding glycine residues in HNCACB/CBCA(CO)NH spectra.

Figure S3

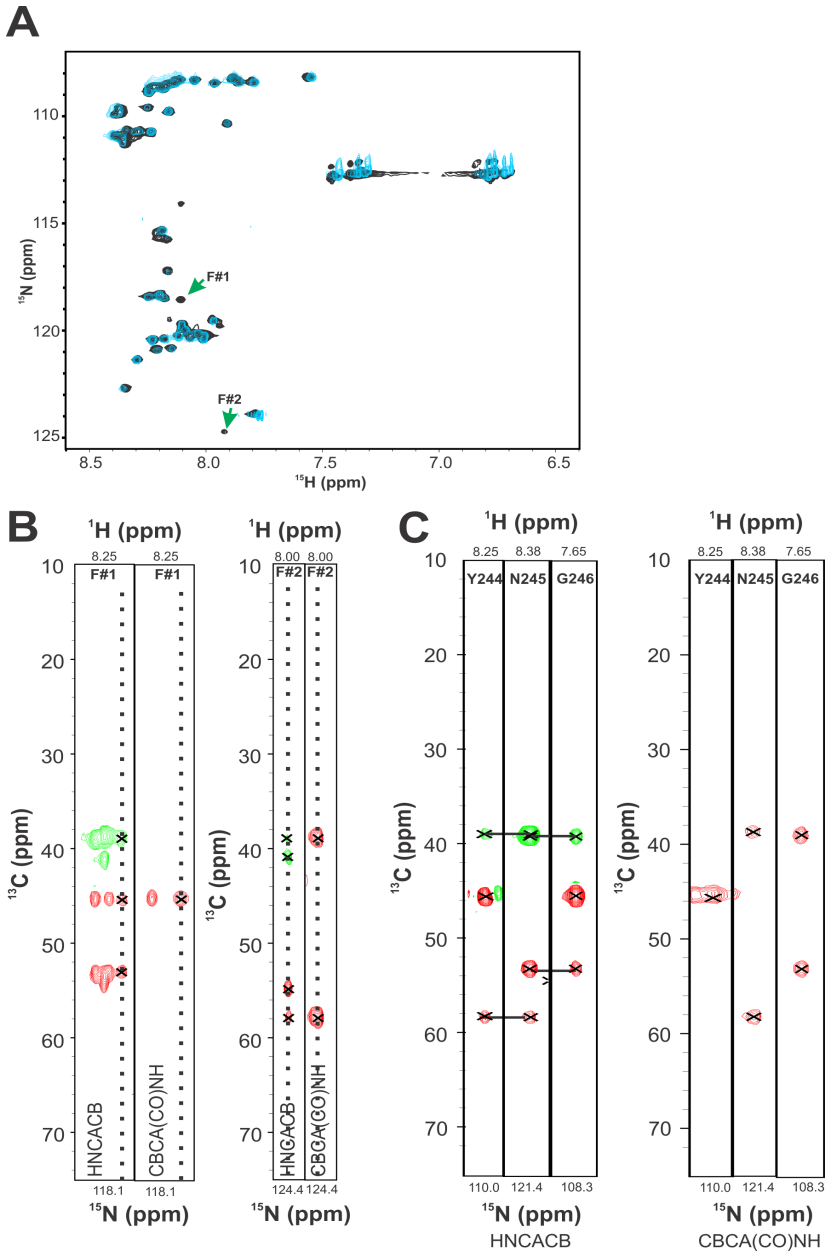

SI Figure 3. Identification of the phenylalanine and tyrosine residues from selectively ^{15}N unlabeled sample of the RGG-box. **(A)** ^{15}N -^{1}H HSQC spectra of selectively Phe unlabeled ^{15}N RGG-box spectra overlaid on ^{15}N-^{1}H HSQC spectra of ^{15}N uniformly labeled RGG-box. **(B)** HNCACB and CBCA(CO)NH strip plots of identified Phe residues (F#1 and F#2). **(C)** HNCACB and CBCA(CO)NH strip plots showing the assignment of Y244, N245, G246 residues of the RGG-box.

Figure S4

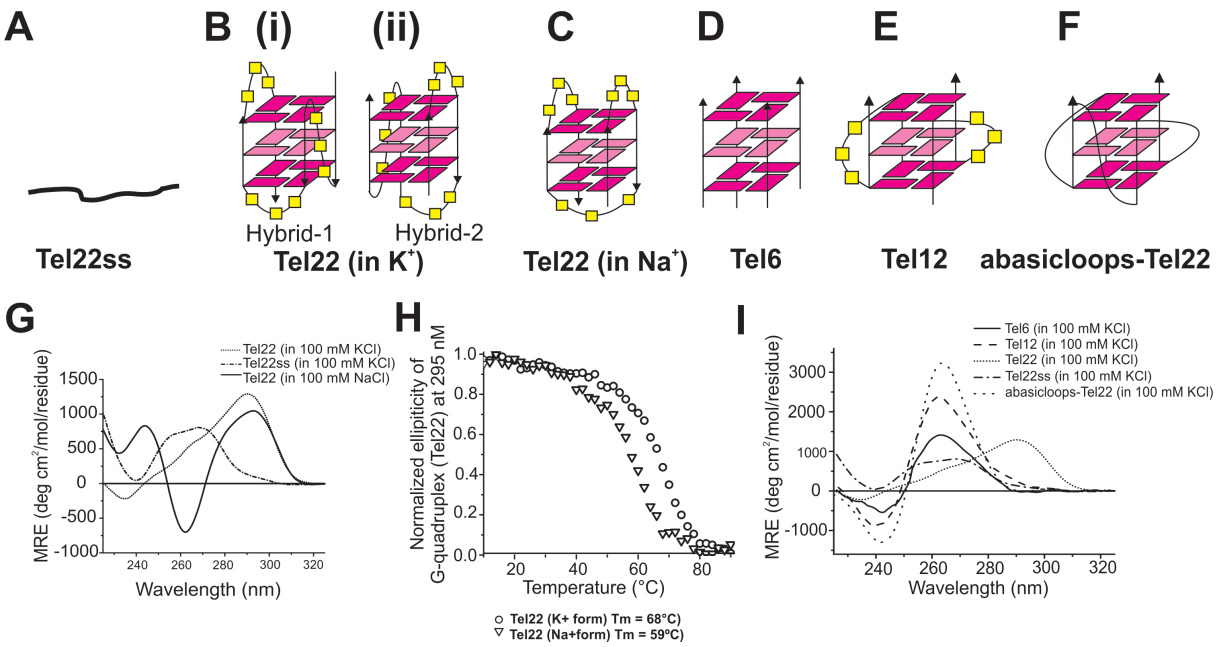

SI Figure 4. Structural characterization of DNA sequences by CD spectroscopy. **(A-F)** Cartoon representation of single stranded Tel22ss **(A),** Tel22 intramolecular G-quadruplex in KCl (**B (i) and (ii)**), Tel22 intramolecular G-quadruplex in NaCl (**C**), Tel6 tetrameric G-quadruplex in KCl (**D**), Tel12dimeric G-quadruplex in KCl (**E**), and abasicloops-Tel22 intramolecular G-quadruplex in KCl **(F**). **(G)** CD spectra of Tel22ss and Tel22 in the presence of 100 mM NaCl and KCl. The Na^+ form of Tel22 shows positive peaks at 295 nm and 245 nm and a negative peak at 265 nm. The K^+ form of Tel22 shows maxima at 295 nm. Tel22ss does not show any of the characteristic peaks of G-quadruplex formation in either NaCl or KCl. **(H)** CD melting curve of Na^+ and K^+ for of Tel22 G-quadruplex monitored at 295 nm by CD spectroscopy. The melting temperature, T_m deduced for both the forms are mentioned. **(I)** CD spectra of Tel22ss and quadruplexes formed by Tel6, Tel12, Tel22 and abasicloops-Tel22 in 100 mM KCl. Tel22 spectrum is characterized by a positive maxima at 295 nm. K^+ form of Tel6, Tel12 and abasicloops-Tel22 spectra are characterized by positive ellipticity at 260 nm and minima at 240 nm. The spectrum of single stranded Tel22ss is also shown.

Figure S5

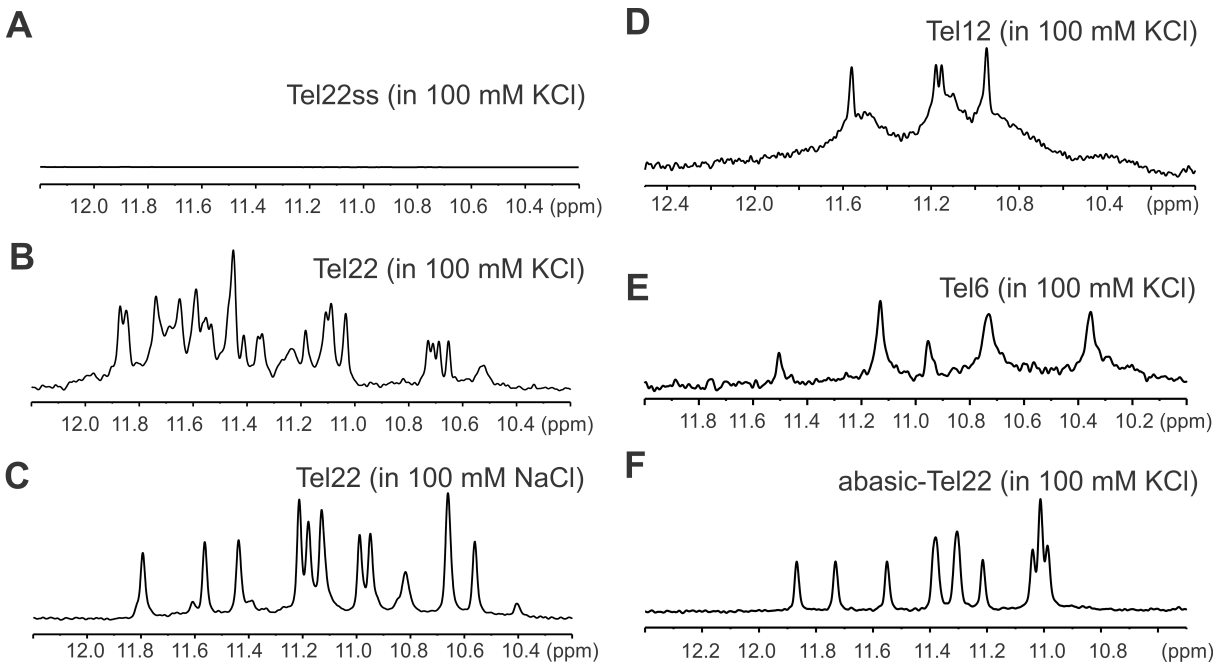

SI Figure 5. Imino region of 1D ^{1}H NMR spectra of DNA used in this study. **(A)** Tel22ss does not show any peak in the imino region, which reinstates the fact that it does not form base-pairs and remains in single stranded conformation. **(B-F)** The imino peaks of G-quadruplex formed byTel22 in 100 mM KCl **(B)**, Tel22 in 100 mM NaCl **(C)**, Tel12 in 100 mM KCl **(D),** Tel6 in 100 mM KCl **(E)** and abasicloops-Tel22 in 100 mM KCl **(F)**.

Figure S6

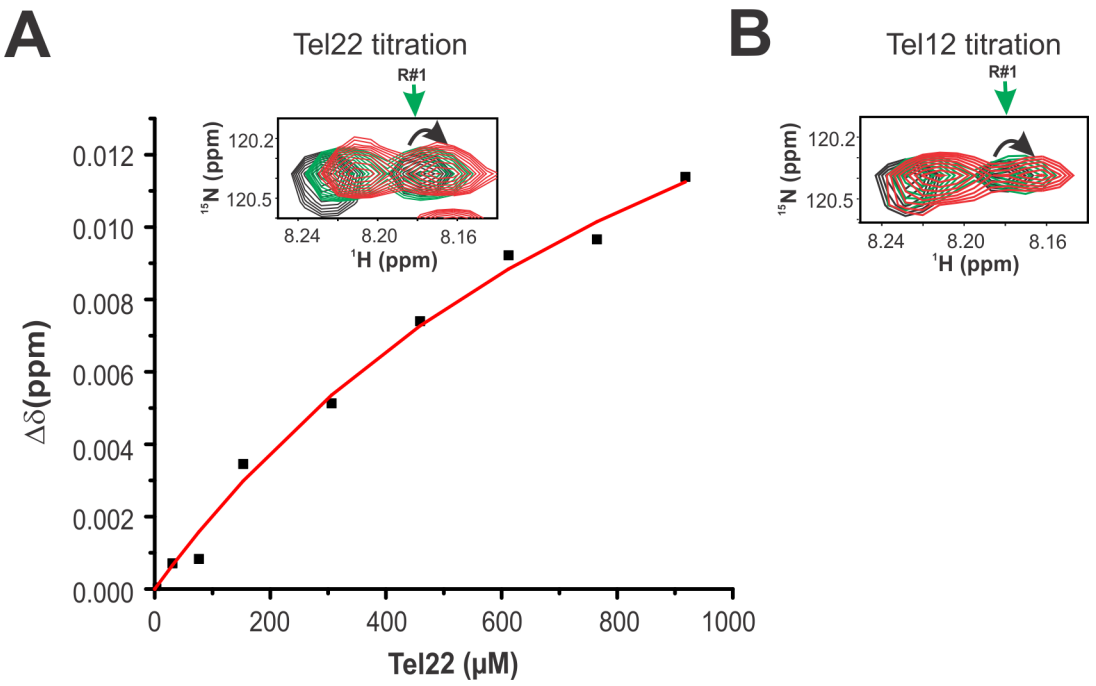

SI Figure 6. Arginine residue R#1 undergoes weak chemical shift perturbation upon binding to Tel22 **(A, inset)** and Tel12 **(B)**. The CSPs observed versus added Tel22 DNA concentration for R#1 is plotted. An apparent individual fit K_d of 913.13±33.92 μM was calculated from this fitting.

Figure S7

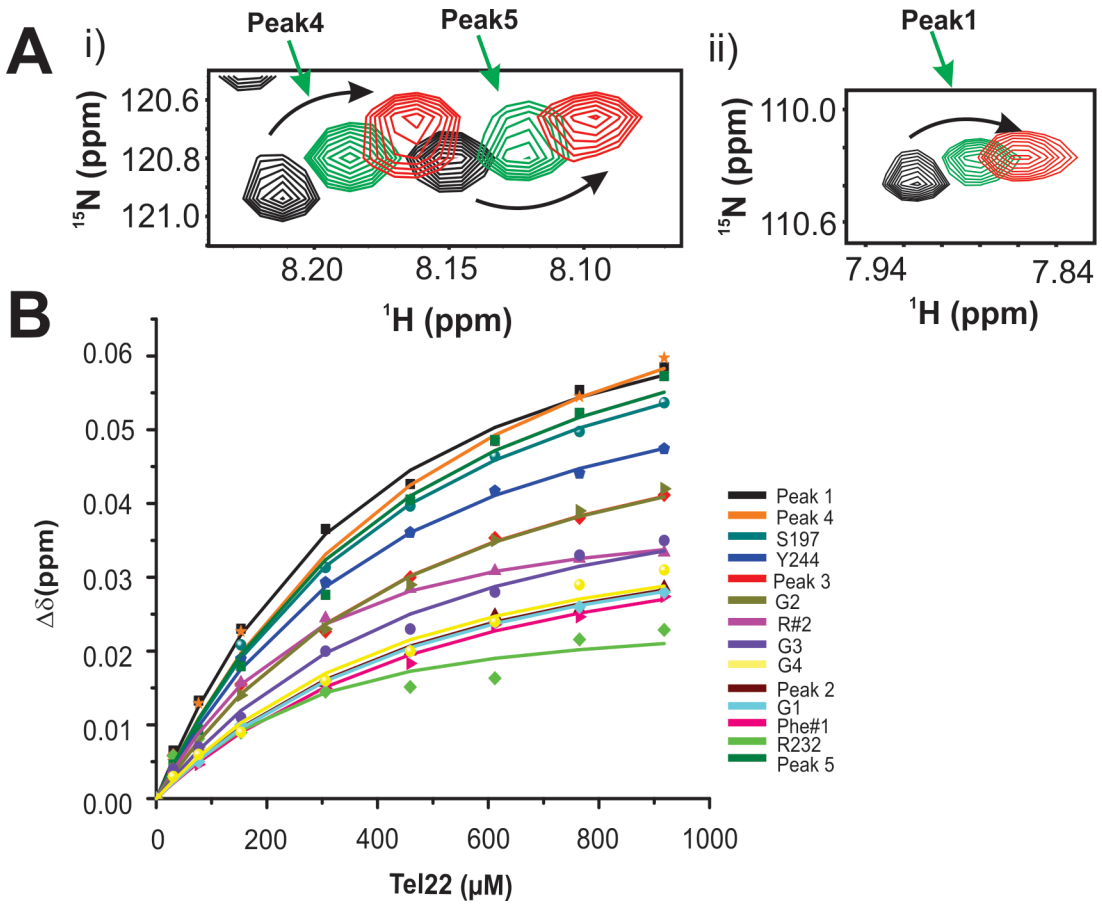

SI Figure 7. A subset of unassigned residues of the RGG-box that shows specific fast exchange chemical shift perturbations upon addition of Tel22DNA (**A (i) and (ii)**). **(B)** The CSPs of the residues used for the calculation of the global fit K_d are plotted as a function of added Tel22 DNA.

Figure S8

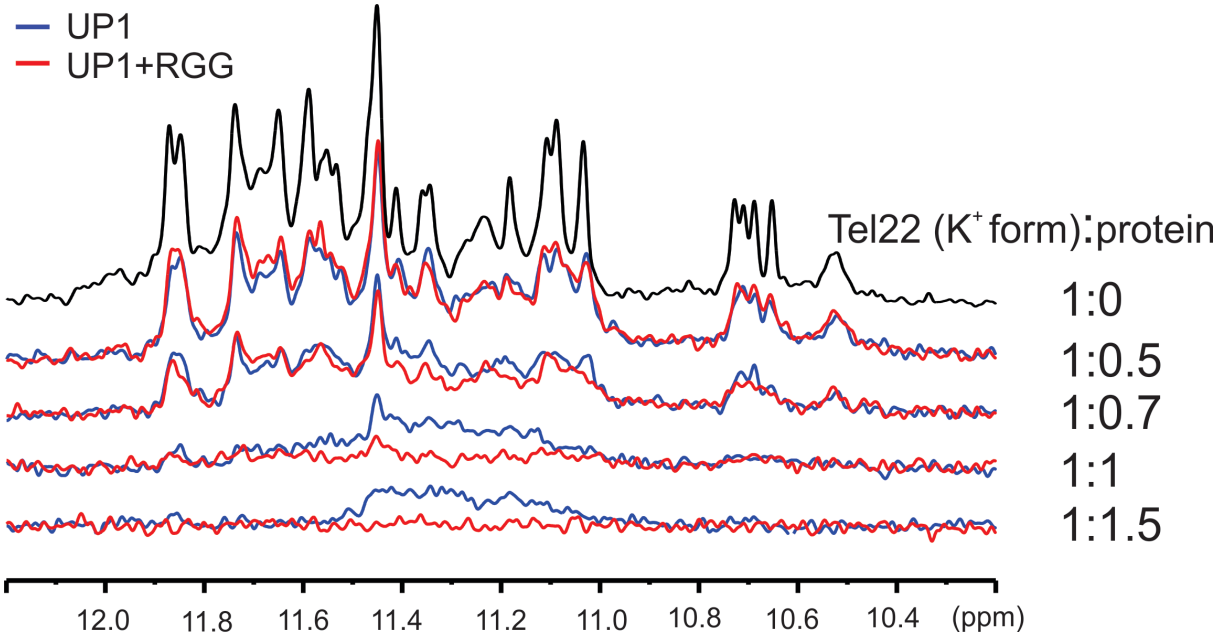

SI Figure 8. Titration of K^+ form of Tel22 with UP1 and UP1+RGG and monitored through NMR spectroscopy. Imino region of the 1D ^1H NMR spectra of K^+ form of Tel22 are shown at varying DNA to protein ratios. The DNA was titrated with increasing concentration of UP1 (blue) and UP1+RGG (red).

Figure S9

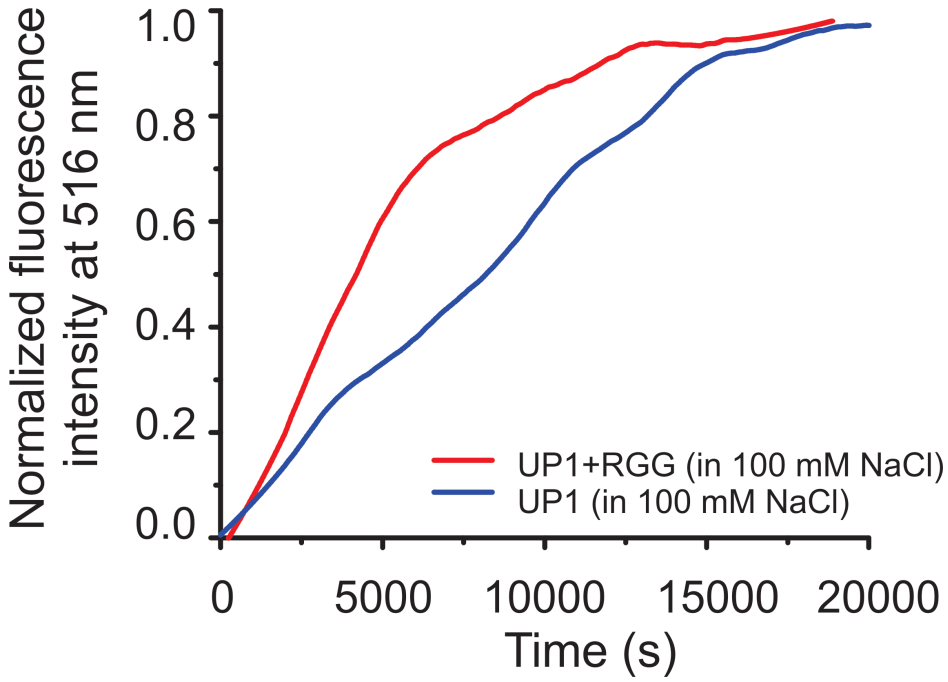

SI Figure 9. Unfolding of the 5'-FAM and 3'-TAMRA labeled Na^+ form of Tel22 (5'FAM-Tel22-TAMRA3') by UP1 (blue) and UP1+RGG (red) monitored by observing the emission of FAM at 516 nM. 5'FAM-Tel22-TAMRA3' DNA was mixed with 4 molar equivalent of UP1 or UP1+RGG and the emission spectra were recorded over a time period. UP1+RGG proceeds with an unfolding rate of k_{obs}= (1.93±0.01) ×10^{-4} s^{-1} and UP1 proceeds with an unfolding rate of k_{obs}= (0.63±0.01) ×10^{-4} s^{-1}, calculated from a single exponential fit of the data in Origin 9.0.

Supplementary Table S1. Individual fit dissociation constant (K_d) values determined for residues of the RGG-box for its interaction with Tel22 G-quadruplex DNA based on the observed chemical shift perturbations.

Sl. No.	***Residues***	***Individual fit K_d (in μM)***
1	Peak1	263.89±9.19
2	Peak2	399.43±13.72
3	Peak3	375.07±15.49
4	Peak4	406.1±15.9
5	Peak5	349.5±19.7
6	F#1	432.86±15.56
7	S197	346.49±10
8	R232	171.81±34.36
9	Y244	305.18±12.926
10	R#2	150.76±7.31
11	G#1	404.96±7.81
12	G#2	377.23±9.89
13	G#3	348.67±18.08
14	G#4	342.60±23.44
Global fit K_d for all these residue: 349±35 μM		